用以發展高效能與低能耗積體電路科技之
高介電氧化物/砷化銦鎵金氧半場效電晶體

(High-κ/InGaAs MOSFETs for High Performance and Low Power IC Technology)

林宗達
國立清華大學　材料科學工程學系　博五
指導教授：**洪銘輝** 博士 與 **郭瑞年** 博士

ABSTRACT

High κ gate dielectrics on channel materials with high carrier mobility are urgently demanded for achieving *high performance* and *low power* complementary metal-oxide-semiconductor (CMOS) technologies beyond the 15 nm node. In this work, using Al_2O_3/GGO dual-layer gate dielectrics and sputtered TiN metal gates, 1μm-gate-length $In_{0.53}Ga_{0.47}As$ and $In_{0.75}Ga_{0.25}As$ MOS field-effect-transistors (MOSFETs) have demonstrated *record-high* maximum drain current ($I_{D\text{-max}}$) of 1.05 mA/μm, peak transconductance ($G_{m\text{-max}}$) of 714 μS/μm, and a high mobility (μ_{FE}) of 1300 cm²/V·s, and $I_{D\text{-max}}$ of 1.23 mA/μm, $G_{m\text{-max}}$ of 464 μS/μm, and μ_{FE} of 1600 cm²/V·s, respectively.

Device Structure and Fabrication

High-κ/InGaAs hetero-structures were prepared in a multi-chamber molecular-beam-epitaxy (MBE)/analysis system, shown in Fig. 1(a). Al_2O_3/$Ga_2O_3(Gd_2O_3)$ [GGO] bi-layer gate dielectrics were e-beam evaporated onto InGaAs in the system. After a post deposition annealing, the gate oxides were covered with TiN using reactive-sputtering from a pure Ti target in Ar/N_2 RF-plasma. The devices, with their schematic cross-section shown in Fig. 1(b), were subsequently fabricated using a self-aligned process.

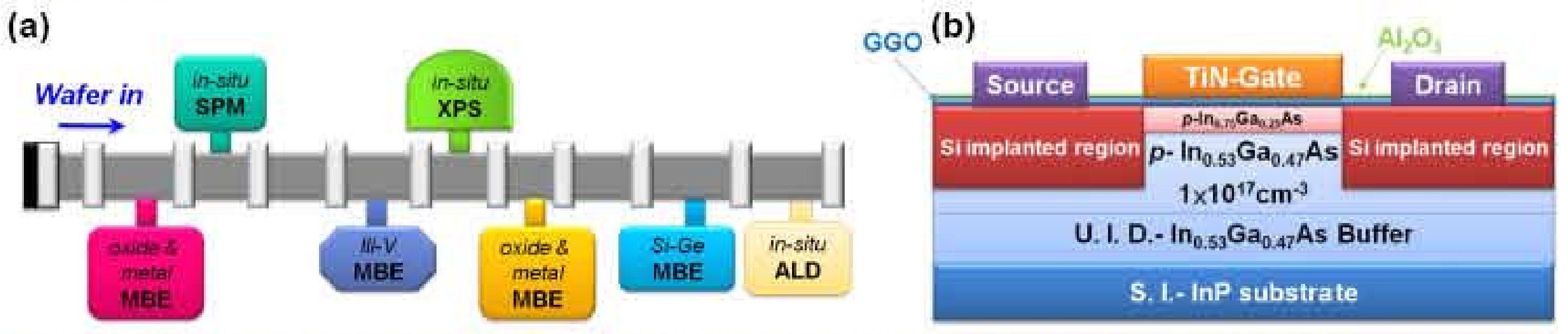

Fig. 1 Schematic diagrams of (a) the multi-chamber MBE/analysis system (b) cross-section of InGaAs *n*-MOSFETs with TiN metal gate and UHV-Al_2O_3/GGO dielectrics.

Results and Discussion

I. dc performance

Figure 2 shows the dc characteristics of the self-aligned inversion-channel Al_2O_3/GGO/InGaAs MOSFETs with gate length of 1 μm. The $In_{0.53}Ga_{0.47}As$ MOSFETs have demonstrated a maximum drain current of 1.05 mA/μm (Fig. 2(a)), peak transconductance of 714 μS/μm (Fig. 2(b)), and a peak field-effect electron mobility of 1300 cm²/V·s (Fig. 2(e)). Moreover, $In_{0.75}Ga_{0.25}As$ MOSFETs, also with a gate length of 1 μm, have achieved a maximum drain current of 1.23 mA/μm (Fig. 2(c)), a peak transconductance of 464 μS/μm (Fig. 2(d)) and a high mobility of 1600 cm²/V·s (Fig. 2(f)).

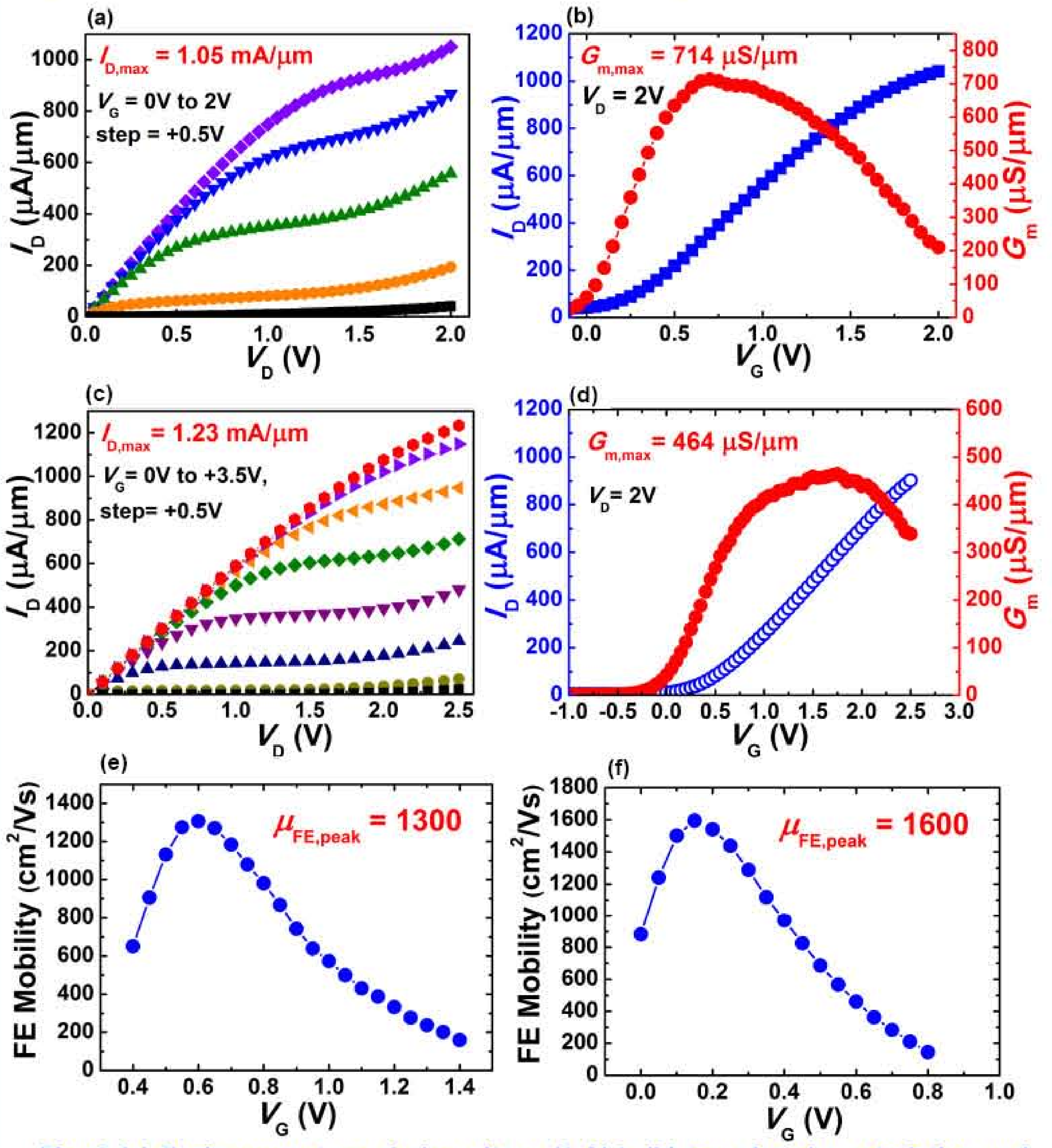

Fig. 2 (a) Drain current vs. drain voltage (I_D-V_D), (b) transfer characteristics and transconductance (G_m), and (e) field-effect mobility (μ_{FE}) of the Al_2O_3/GGO/$In_{0.53}Ga_{0.47}As$ MOSFET. (c) I_D-V_D curve, (d) transfer characteristics and G_m curve, and (f) μ_{FE} of the Al_2O_3/GGO/$In_{0.75}Ga_{0.25}As$ MOSFET.

II. rf performance

The Al_2O_3/GGO/$In_{0.53}Ga_{0.47}As$ MOSFETs (L_G = 1 μm; W_G = 10 μm) have also exhibited outstanding embedded rf characteristics (Fig. 3(a)), including a cutoff frequency (f_T) of 17.9 GHz and a maximum frequency of oscillation (f_{max}) of 11.2 GHz. Both the f_T and f_{max} show very minor change with varying gate bias (Fig. 3(b)), which is highly preferred for circuit applications.

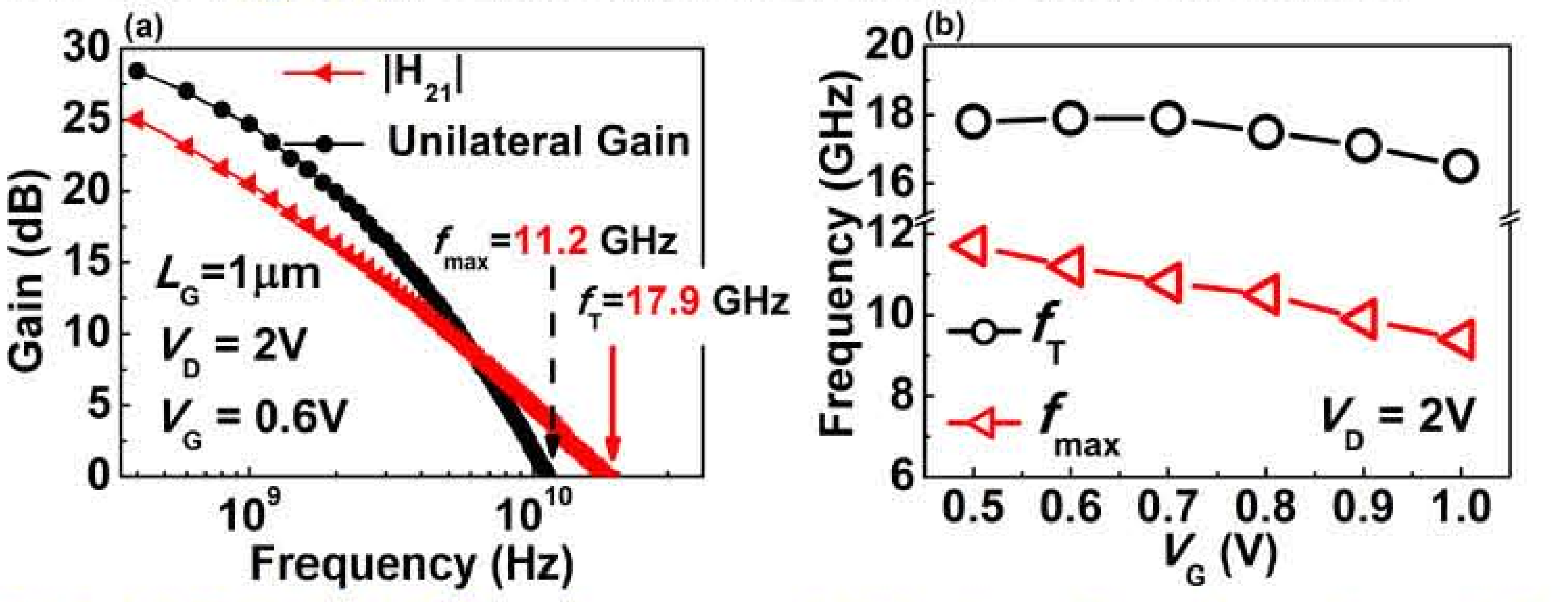

Fig.3 (a) Embedded RF performance and (b) gate voltage dependence of the frequency responses of the $In_{0.53}Ga_{0.47}As$ MOSFET.

III. E-mode InGaAs MOSFETs — Benchmarking

$I_{D\text{-max}}$ and $G_{m\text{-max}}$ of representative E-Mode (inversion-channel or non inversion-channel) InGaAs MOSFETs (with $L_G \leq$ 1 μm) are summarized and favorably compared in Fig. 4(a) and (b), respectively. The $I_{D\text{-max}}$ demonstrated by the inversion-channel Al_2O_3/GGO/InGaAs MOSFETs are the highest ever achieved among all E-mode InGaAs MOSFETs; the $G_{m\text{-max}}$ of 714 mS/μm achieved in the Al_2O_3/GGO/$In_{0.53}Ga_{0.47}As$ MOSFETs was the record-value and it is still the highest among E-mode InGaAs MOSFETs with $L_G \geq$ 0.2 μm.

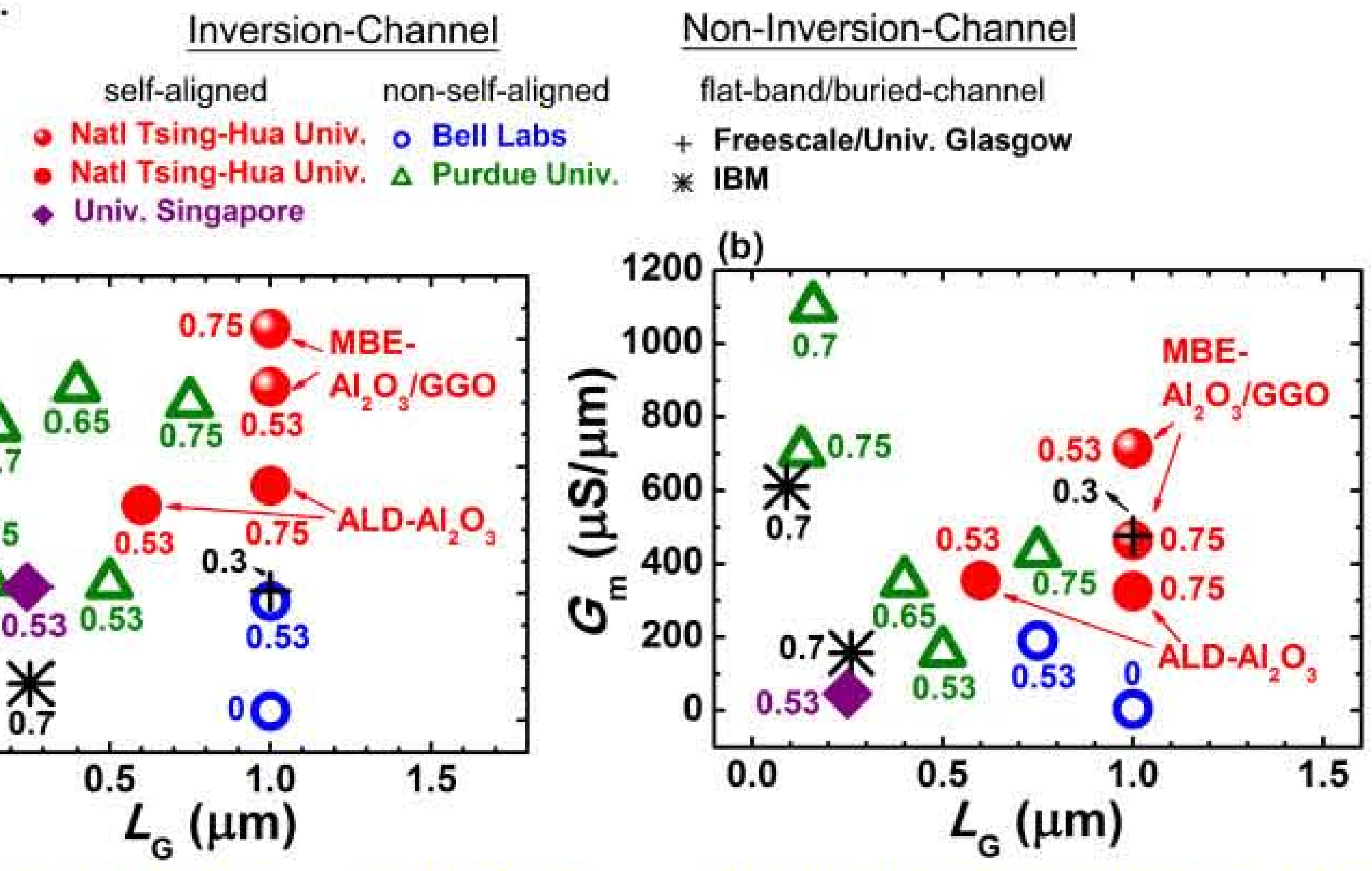

Fig. 4 Summary of (a) $I_{D\text{-max}}$ and (b) $G_{m\text{-max}}$ of representative work on III-V enhancement-mode *n*-MOSFETs reported in the last decade. The number near each data point indicates the In content (x) of the $In_xGa_{1-x}As$ channel used in corresponding device; x=0 stands for a GaAs channel. The self-aligned processed inversion-channel devices are denoted with solid circular and diamond symbols, and the data of non-self-aligned processed inversion-channel devices are denoted with hollow circular and triangular symbols. Symbols of cross and stars represent the data of non-inversion-channel (flat-band type or buried channel) E-mode MOSFETs.

Conclusion

The Al_2O_3/GGO/InGaAs MOSFETs have set records, not only for III-V MOSFETs but also for all enhancement-mode MOSFETs with similar gate-lengths, regardless of channel materials and device configurations. This work has shown that the high-κ's with InGaAs indeed produce much higher drain currents and transconductances than those of Si MOSFETs, and may be the key for realizing ultimately scaled planar device with high performance and low power consumption.

The author has devoted himself to realizing high performance inversion-channel InGaAs MOSFETs for six years. He feels excited to carry out such an important and challenging research project.

財團法人中技社 99年度 「科技獎學金」